



Published in final edited form as:

Genes Brain Behav. 2012 February ; 11(1): 62–68. doi:10.1111/j.1601-183X.2011.00733.x.

Preliminary evidence of abnormal white matter related to the fusiform gyrus in Williams syndrome: A diffusion tensor imaging tractography study

Brian W. Haas, PhD¹, Fumiko Hoefft, MD PhD¹, Naama Barnea-Goraly, MD¹, Golijeh Golarai, PhD², Ursula Bellugi, Psy.D³, and Allan Reiss, MD^{1,CA}

¹Center for Interdisciplinary Brain Sciences Research (CIBSR), Stanford University School of Medicine, 401 Quarry Rd. Palo Alto, CA USA 94305-5795

²Department of Psychology, Stanford University, Palo Alto, CA USA 94305

³Laboratory for Cognitive Neuroscience, Salk Institute for Biological Studies, 10010 N. Torrey Pines Road, La Jolla, CA 92037

Abstract

Williams syndrome is a genetic condition caused by a hemizygous microdeletion on chromosome 7q11.23. Williams syndrome is characterized by a distinctive social phenotype comprised of increased drive towards social engagement and attention towards faces. Additionally, individuals with Williams syndrome exhibit abnormal structure and function of brain regions important for the processing of faces such as the fusiform gyrus. This study was designed to investigate if white matter tracts related to the fusiform gyrus in Williams syndrome exhibit an abnormal structural integrity as compared to typically developing (age matched) and developmentally delayed (IQ matched) controls. Using diffusion tensor imaging data collected from forty (20 Williams syndrome, 10 typically developing and 10 developmentally delayed) participants, white matter fibers were reconstructed that project through the fusiform gyrus and two control regions (caudate and the genu of the corpus callosum). Macro-structural integrity was assessed by calculating the total volume of reconstructed fibers and micro-structural integrity of reconstructed fibers was assessed by calculating fractional anisotropy and fiber density index. Williams syndrome participants, as compared to controls, exhibited an increase in the volume of reconstructed fibers and an increase in fractional anisotropy and fiber density index for fibers projecting through the fusiform gyrus. No between-group differences were observed in the fibers that project through the control regions. Although preliminary, these results provide further evidence that the brain anatomy important for processing faces is abnormal in Williams syndrome.

Keywords

Williams syndrome; genetics; DTI; fusiform; tractography

^{CA}Corresponding Author: Allan L. Reiss, Center for Interdisciplinary Brain Sciences Research, Stanford University School of Medicine, 401 Quarry Road, Stanford, CA 94305-5719, USA. areiss1@stanford.edu.

Introduction

Williams syndrome (WS) is a neurodevelopmental condition caused by a hemizygous microdeletion on chromosome 7q11.23. WS is characterized by a distinctive social phenotype characterized by hypersociability, social disinhibition and increased attention towards faces. For example, as compared to chronologically and mentally age-matched controls, individuals with WS rate photographs of facial expressions as more approachable (Jones *et al.*, 2000), approach others such as strangers more frequently (Doyle *et al.*, 2004), and fixate on faces longer (Riby *et al.*, 2010). Together, these findings lend support to the hypothesis that WS is associated with abnormalities in brain regions important for social-cognitive functioning and in particular the processing of facial expressions (Martens *et al.*, 2008).

One brain region particularly important for the processing of social information conveyed through facial expressions is the fusiform gyrus. The fusiform gyrus contains the fusiform face area (FFA), which is a highly specialized region for face recognition (Kanwisher *et al.*, 1997). For example, BOLD activation within the FFA correlates with the ability to detect the presence of faces (Grill-Spector *et al.*, 2004), and damage to the FFA, as in acquired prosopagnosia, results in a compromised ability to recognize facial expressions (Barton, 2008). Recently, evidence has emerged that WS is associated with structural and functional abnormalities within the fusiform gyrus. Individuals with WS exhibit greater cortical gray-matter thickness (Thompson *et al.*, 2005) and reduced gray matter volume of the fusiform gyrus (Campbell *et al.*, 2009) and greater volume of the functionally-defined FFA within the fusiform gyrus (Golarai *et al.*, 2010). In spite of evidence of structural and functional abnormalities within the fusiform gyrus in WS, very little is known regarding alterations of white matter related to the fusiform gyrus in WS.

This study was designed to investigate the integrity of white matter fibers that project through the fusiform gyrus in WS by using a Diffusion Tensor Imaging (DTI) tractography approach. DTI is a neuroimaging technique that is particularly advantageous for elucidating the structural integrity of white matter within the living human brain based on measurements of water diffusion. DTI *tractography* integrates this information to infer connectivity patterns associated with *a priori* defined regions of the brain (Lazar, 2010). Thus, DTI tractography is a particularly useful tool to infer patterns of brain connectivity in both normal and pathological conditions.

Based on evidence that WS is associated with abnormalities in face processing (Karmiloff-Smith *et al.*, 2004, Leonard *et al.*, 2011) and with abnormalities in the gray matter structure (Campbell *et al.*, 2009, Thompson *et al.*, 2005) and function (Golarai *et al.*, 2010) of the fusiform gyrus, we predicted that WS is associated with abnormalities in the white matter tracts related to the fusiform gyrus. We tested this hypothesis by reconstructing white matter fibers that project through the fusiform gyrus in a sample of WS subjects as compared to two control groups: Typically Developing (TD), and Developmentally Delayed (DD). In order to examine the anatomical specificity of white matter abnormalities in WS, we also reconstructed white matter fibers that project through two other regions; the caudate and the genu of the corpus callosum.

Methods

Participants

A total of 40 individuals, 20 WS, 10 TD and 10 DD, participated in the study. Twenty WS participants (9 females: mean age = 28.19, SD = 9.55; mean IQ = 63.21; 18 right-handed) were recruited. All genetic diagnoses were confirmed using florescent in situ hybridization (FISH) probes for elastin (ELN), a gene consistently found in the microdeletion associated with WS. All participants exhibited the medical and clinical features of the WS phenotype, including cognitive, behavioral, and physical profiles.

TD subjects were recruited locally (Palo Alto, CA) and were financially compensated for their participation (10 total: 2 females; mean age = 27.77, SD = 9.53, mean IQ = 114.33: 10 right-handed). TD subjects were screened for a history of psychiatric or neurologic problems using the Symptom Checklist-90-R (SCL-90-R) (Derogatis, 1977). All subjects had SCL-90-R scores that fell within one SD of a normative sample.

Criteria for the DD control group were met if participants' full-scale intelligence quotient (IQ) fell below one SD of the norm and participants did not have the diagnosis of WS (10 total: 7 females; mean age = 23.71, SD = 5.30; mean IQ = 70.9; 8 right-handed). Among the DD individuals, seven had idiopathic DD, and three had a diagnosis of fragile X syndrome, Turner syndrome, and velocardiofacial syndrome.

The WS group exhibited a lower mean full scale IQ as compared to the TD group ($t(1, 28) = 8.83, p < .001$). However, there was no statistically significant difference in the mean full scale IQ between the WS and the DD groups ($t(1, 28) = 1.54, p = .14$). Furthermore, there were no statistically significant differences in age between the WS and TD groups ($t(1, 28) = .11, p = .91$), the DD and WS groups ($t(1, 18) = 1.37, p = .18$) or the DD and TD groups, ($t(1, 18) = 1.18, p = .25$). Lastly, there was no significant difference in gender between experimental groups ($F(2, 37) = 2.67, p = .082$).

No participants had a contra-indication for MRI and written informed consent and/or assent were obtained from each participant. This study was approved by the Stanford University Administrative Panel on Human Subjects in Medical Research.

DTI Image Acquisition

Magnetic resonance images of each subject's brain were acquired at the Richard M. Lucas Center for Imaging (Stanford University, Palo Alto, CA USA) using a 3T Signa LX (GE Medical Systems, Milwaukee, WI USA). A DTI sequence was based on a single-shot spin-echo echoplanar imaging sequence with diffusion sensitizing gradients applied on both sides of the 180° refocusing pulse (Basser *et al.*, 1994). Imaging parameters for the diffusion-weighted sequence were as follows: field of view (FOV), 24 cm; matrix size, 128 × 128 (33 slices); echo time (TE), 60.4 ms; repetition time (TR), 12200 ms; 33 axial-oblique slices; slice thickness, 3.8 mm/skip 0.4 mm. Diffusion gradient duration was $\Delta = 32$ ms, and diffusion weighting was $b = 815$ s/mm². In addition, two reference measurements (b_0 scans) having no diffusion sensitizing gradients were performed and averaged for each slice. Diffusion was measured along 12 diffusion directions (6 noncollinear directions: XY, XZ,

YZ, -XY, -XZ, and -YZ). In order to obtain an appropriate signal to noise ratio, this pattern was repeated six times for each slice, with the sign of all diffusion gradients inverted for odd repetitions. Data were then averaged across all six repetitions. In order to delineate regions of interest (seeds) used for fiber tracking, a high-resolution, three-dimensional T1-weighted anatomic gradient, receptive field spoiled-gradient scan (SPGR), MRI sequence with the following parameters was used: TR = 35 ms; TE = 6 ms; flip angle = 45°; number of excitations, 1; matrix size = 256 × 256; FOV = 24 cm²; 124 contiguous slices of 1.5mm-thickness image was collected for each subject.

DTI Image Processing

Diffusion-weighted images were corrected for eddy current distortions and head motion using linear image registration (Automated Image Registration (AIR) algorithm) (Woods *et al.*, 1998). Thereafter, DtiStudio (Jiang *et al.*, 2006) (<https://www.dtistudio.org/>) was used. All individual images were visually inspected to discard slices with motion artifacts, and the remaining images were averaged for each slice. There were no statistical differences in the proportion of discarded slices between-groups ($p > .10$). The pixel intensities of the multiple diffusion-weighted images were fitted to obtain all elements of the symmetric diffusion tensor. The diffusion tensors at each pixel were diagonalized to obtain pixel eigenvalues and eigenvectors. Fractional anisotropy (FA) maps, average non-diffusion weighted images ($b = 0$ s/mm²) were retained.

Diffusion-Tensor Fiber-Tracking

Fiber-tracking was performed using the Fiber Assignment by Continuous Tracking (FACT) method (Mori *et al.*, 1999). Briefly, tracing was initiated from a seed voxel from which a line was propagated in both retrograde and orthograde directions according to eigenvector (v1) at each voxel. The tracking was terminated when it reached a voxel with an FA value lower than 0.15 (Wakana *et al.*, 2004), or when the turning angle was greater than 70° (Roberts *et al.*, 2005). In order to reconstruct branching patterns, the tracking was performed from every voxel inside the brain, but only fibers that penetrated *a priori* defined ROIs were retained.

Fusiform ROIs were outlined manually by reliable raters (intraclass interrater reliability >0.9), on positionally normalized brain image stacks in a coronal orientation perpendicular to the horizontal plane defined by the anterior and posterior commissures. The definition of the fusiform gyrus ROI included the gray and white matter between the lateral occipito-temporal sulcus, and the lateral bank of the collateral sulcus (Figure 1A). The anterior extent of the fusiform gyrus was defined by the coronal slice that intersected the posterior edge of the amygdala. The posterior extent of the fusiform gyrus was defined by the last coronal slice that included a white matter tract (Duvernoy, 1999).

As control regions, ROIs were delineated to encompass the left and right caudate and the genu of the corpus callosum. The caudate ROIs were delineated using a knowledge-driven algorithm to delineate the caudate nucleus for each participant (Xia *et al.*, 2007). This method has been shown to be reliable and to produce volumes that are suitable to detect condition-specific alterations in volume and in white matter tracts related to the caudate (Haas *et al.*, 2009). The genu ROI was delineated by using a standardized circle ROI with a

diameter of 10 voxels. The ROI was positioned on each participant's most medial sagittal slice using a color map (DTI data), where the entire corpus callosum was most clearly visualized in red.

Measurements of total, gray and white volumes were calculated for the fusiform and caudate ROIs. Gray and white matter tissue types were segmented using a probabilistic tissue segmentation algorithm (Reiss *et al.*, 1998) available within the program, BrainImage v5.x (Reiss, 2011). The fusiform gyrus, as defined in this study includes both gray and white matter, while the caudate is comprised almost entirely of gray matter. Therefore, for the fusiform gyrus, we separately entered gray and white matter as covariates into our statistical model, and for the caudate we entered total tissue volume as a covariate into our statistical model. We carried out these procedures in order to ensure that group differences in tissue volume were not affecting the DTI results.

The fusiform and caudate ROIs were aligned to DTI space by using a rigid body (affine) transformation. Spatial alignment was carried out by obtaining parameters derived from the coregistration from each participant's SPGR image to each participant's mean b0 image (DTI data) and applying the parameters to each ROI.

Each ROI was used as a seed region in DTI space within DTIstudio (Figure 1B). White matter fibers were selected if they projected through each *a priori* defined ROI (left and right fusiform gyrus, left and right caudate and genu). For each fiber tract bundle, metrics indicative of macro and micro-structure were collected. Macro-structure was quantified by the total volume of each reconstructed fiber bundle. Micro-structure metrics included fractional anisotropy (FA) and fiber density index (FDi).

A priori statistical analyses were initiated by conducting a repeated measures ANOVA with group (WS vs. TD vs. DD) entered as a between subjects factor and side (left versus right, for fusiform and caudate) as the within subjects factor. Each ANOVA comparing macro-structure was also conducted while controlling for total (caudate), gray (fusiform) and white (fusiform) matter volumes. Under the scenario that a significant effect of group was observed (WS vs. TD vs. DD) we examined main effects using each control group (WS vs. TD and WS vs. DD independently) and simple effects targeting each side (left and right independently) for each DTI metric.

Results

Fusiform: Volume of reconstructed white matter tracts

Probabilistic maps of reconstructed white matter tracts for each group are displayed in Figure 2. We conducted a repeated measures ANOVA using the volume of reconstructed fibers that project through the fusiform with group (WS vs. TD vs. DD) as the between subjects factor and hemisphere (left vs. right) as the within subjects factor. This analysis revealed a significant effect of group $F(2, 37) = 7.091, p = .002$, and no significant effect of hemisphere $F(2, 37) = .009, p = .92$ (Figure 3A). The effect of group remained significant when gray and white matter ROI volumes were entered as covariates, gray: $F(2, 36) = 10.45, p < .001$; white: $F(2, 36) = 7.00, p = .003$.

We next compared the volume of reconstructed fibers that project through the left and right fusiform independently between the WS group and each of the control groups. The WS group, as compared to the TD group, exhibited a greater volume of reconstructed fibers that project through the left $t(1, 28) = 2.80, p < .01$, and right fusiform $t(1, 28) = 2.39, p < .05$. The WS group, as compared to the DD group, also exhibited a greater volume of reconstructed fibers that project through the left $t(1, 28) = 2.74, p < .05$, and right fusiform $t(1, 28) = 2.49, p < .05$. No statistically significant differences in volume of reconstructed fibers that project through the fusiform were observed between the TD and DD control groups.

Fusiform: Fractional Anisotropy

We conducted a repeated measures ANOVA using the FA of reconstructed fibers that project through the fusiform with group (WS vs. TD vs. DD) as the between subjects factor and hemisphere (left vs. right) as the within subjects factor. This analysis revealed a significant effect of group $F(2, 37) = 3.97, p < .05$, and no significant effect of hemisphere $F(2, 37) = 1.51, p = .23$ (Figure 3B).

We next compared the FA of reconstructed fibers that project through the left and right fusiform independently between the WS group and each of the control groups. The WS group, as compared to the TD group, exhibited greater FA of reconstructed fibers that project through the left $t(1, 28) = 2.09, p < .05$, and right fusiform $t(1, 28) = 2.70, p < .01$. However, the differences between the WS and DD groups did not reach statistical significance though the right side approached significance (left: $t(1, 28) = 1.03, p = .31$; right: $t(1, 28) = 1.76, p = .09$). No statistically significant differences in FA of reconstructed fibers that project through the fusiform were observed between the TD and DD control groups.

Fusiform: Fiber Density

For each fiber bundle, the mean number of reconstructed fibers per voxel was calculated (termed Fiber Density Index: FDi). We conducted a repeated measures ANOVA on the FDi of reconstructed fibers that project through the fusiform with group (WS vs. TD vs. DD) as the between subjects factor and hemisphere (left vs. right) as the within subjects factor. This analysis revealed a significant effect of group $F(2, 37) = 8.46, p = .001$ and no significant effect of hemisphere $F(2, 37) = .88, p = .35$ (Figure 3C).

We next compared the FDi of reconstructed fibers that project through the left and right fusiform independently between the WS group and each of the control groups. The WS group, as compared to the TD group, exhibited greater FDi of reconstructed fibers that project through the left $t(1, 28) = 3.34, p < .005$, and right fusiform $t(1, 28) = 2.06, p < .05$. The WS group, as compared to the DD group exhibited greater FDi of reconstructed fibers that project through the left $t(1, 28) = 3.00, p < .01$, and right fusiform $t(1, 28) = 2.67, p < .05$. No statistically significant differences in FDi of reconstructed fibers that project through the fusiform were observed between the TD and DD control groups.

Control regions: All DTI metrics

We conducted repeated measures ANOVAs on each of the dependent variables (volume: controlling for caudate ROI total tissue volume, FA and FDi) related to the reconstructed fibers projecting through the caudate and the genu of the corpus callosum with group (WS vs. TD vs. DD) as the between subjects factor and side (for the caudate) as the within subjects factor. These analyses revealed no significant effects of group or side for the caudate or the genu (all p 's > .10).

Discussion

In this study, we demonstrate that WS is associated with abnormal anatomy of white matter fibers projecting through the fusiform gyrus. This finding is consistent with prior research showing that individuals with WS process facial expressions differently as compared to chronologically and mentally aged-matched controls (Riby *et al.*, 2010) and with prior research showing that WS is associated with alterations in gray matter structure (Campbell *et al.*, 2009, Thompson *et al.*, 2005) and function (Golarai *et al.*, 2010) within the fusiform gyrus. Together, these studies indicate that WS may be associated with abnormal development of brain anatomy important for the processing of social information and in particular facial expressions.

The current finding of abnormalities of white matter related to the fusiform gyrus may be an underlying neural substrate associated with the social phenotype of WS. As compared to TD controls, those with WS are less socially inhibited (Doyle *et al.*, 2004), more attentive towards facial expressions (Riby *et al.*, 2010), and more likely to rate facial expressions as being approachable (Bellugi *et al.*, 1999). Recently, evidence has emerged suggesting that individuals with WS process faces differently as compared to controls. Specifically, those with WS tend to process faces based on individual features (i.e. eyes and mouth), while healthy controls process faces more holistically (i.e. the whole face combined) (Annaz *et al.*, 2009, Isaac & Lincoln, 2011, Karmiloff-Smith *et al.*, 2004). Taken together, abnormal cognitive processing of faces, along with alterations of brain anatomy including the fusiform gyrus, likely interact and contribute to the WS social phenotype.

The fusiform gyrus exhibits extensive connections with many brain regions including visual processing areas, the frontal lobe and parietal lobe. The fusiform gyrus is also part of a distributed neural system that is highly specialized for face perception (Haxby *et al.*, 2000). For example, the functional connectivity between the fusiform and the superior temporal sulcus and orbital frontal cortex (OFC) is greater when healthy subjects view faces versus scrambled images (Fairhall & Ishai, 2007). Recently, Sarpal and colleagues (2008) demonstrated that individuals with WS exhibit abnormal functional connectivity between the fusiform, amygdala and several portions of the prefrontal cortex during passive viewing of faces versus houses. Our findings extend prior research by showing that the anatomical connections with the fusiform gyrus are structurally abnormal in WS.

In this study, we used a DTI tractography approach to measure white matter macro- and micro-structural integrity. Macro-structural integrity was assessed by calculating the total volume of reconstructed fibers. Micro-structural integrity was assessed by calculating

fractional anisotropy (FA) and fiber density index (FDi). The metrics used here are most likely reflective of different neuroanatomical features. For example, the metric of macro-structure used here (the volume of reconstructed fibers) is not a direct measure of the real volume or number of axons within a particular tract. However, the volume of reconstructed fibers has been used to investigate white matter structural integrity and has been shown to be reduced in clinical conditions characterized by white matter loss such as in cerebral palsy (Thomas *et al.*, 2005) and in those affected by strokes (Schaechter *et al.*, 2008). Further research combining DTI with functional neuroimaging techniques in humans and histological approaches in animals is necessary to elucidate the relationship between increased volume of fibers, functional anatomy and cytoarchitecture.

In terms of micro-structure, FA is a metric indicative of the proportion of linear diffusion (movement) of water molecules in a particular direction. Typically, locations comprised of white matter tissue as compared to other types of tissues within the brain (i.e. gray matter) exhibit higher values of FA. FDi represents the average number of reconstructed fibers per voxel and is thought to be reflective of the density of white matter fibers projecting through a voxel (Roberts *et al.*, 2005, Vernooij *et al.*, 2007).

In this study, diffusion tensors were measured along 12 directions (6 noncollinear directions). Recently, many DTI sequences have been designed to measure diffusion tensors along a greater number of directions relative to the data acquired for this study. Although it has been suggested that performing tractography with more diffusion directions is associated with a reduced likelihood of committing errors related to crossing or “kissing” fibers, a direct comparison of the fidelity of diffusion-weighted data collected using optimized 6, 10, 15 and 30 direction schemes indicates that each have comparable precision and that they each have sufficient power in order to discriminate normal from abnormal white matter integrity (Landman *et al.*, 2007). Furthermore, tractography analyses using diffusion-weighted data with six noncollinear directions has been shown to be effective in dissociating white matter tracts related to autistic spectrum disorders (Sundaram *et al.*, 2008), mental arithmetic skills (Tsang *et al.*, 2009) and face perception (Thomas *et al.*, 2008).

We observed statistically significant differences in both macro and micro-structure between WS and controls. However, in terms of FA, we only observed statistically significant differences between the WS and TD groups and not between the WS and DD groups. The lack of a statistically significant difference in FA between the WS and DD groups may be due to several factors. For example, the DD group, as compared to the WS and TD groups, is relatively more heterogeneous. Among the DD individuals, seven had idiopathic DD, and three had a non-WS diagnosis; of fragile X syndrome, Turner syndrome, and velocardiofacial syndrome. This study was also limited in terms of sample size for the DD group ($n = 10$). It may be the case that if there were a greater number of DD participants (as in the WS group), statistically significant differences may have been observed between the WS and DD group.

In this study, statistically significant differences were found between the WS and control groups in DTI metrics related to the fusiform gyrus, but not in DTI metrics related to other brain regions including the genu of the corpus callosum. Several studies have reported on

structural abnormalities within the corpus callosum in WS, primarily in posterior regions such as the isthmus and splenium (Paul, 2011). Our study used an approach to track white matter fibers related to the most anterior portion of the corpus callosum (genu). Clearly, more research on the structure and function of the corpus callosum in WS is warranted.

The findings presented here indicate that the deleted genes in WS may influence the development of the neuroanatomy involved in processing facial expressions. However the current results are based on data acquired from adults with WS and thus are limited in terms of informing models of neurodevelopment in WS directly. Future studies designed to investigate neuro and behavioral development throughout early childhood in WS will help to elucidate the interaction between genes, environmental factors and social brain function in WS.

Although the results presented here highlight the presence of structural abnormalities of white matter associated with the fusiform gyrus in WS, these results must be taken as preliminary. Social functioning and in particular face processing is abnormal in WS. However, the fusiform gyrus is responsible for many functions (only one of which is face processing). Ideally, this study would have included behavioral data indicative of individual differences in face processing. However, these data were not acquired for a large enough subset within our sample, and thus statistical analyses were not justified. Another approach that would improve the specificity of these findings would be to acquire FFA localizer fMRI scans for each participant (Golarai *et al.*, 2010). As a result, white matter tracts related to the face-processing region within the fusiform could be isolated more accurately. Accordingly, the results presented here should be considered preliminary and hypothesis generating with respect to further investigations of functional and structural aberrations of the fusiform in WS.

Conclusions

In conclusion, we have provided evidence that the white matter tracts associated with the fusiform gyrus exhibit abnormal macro- and micro-structural characteristics in WS as compared to chronologically and mentally age matched controls. This finding provides further support for a model relating genetic risk in WS to structural and functional aberrations within the brain, ultimately influencing the development of distinctive social behaviors in this condition. Clearly, as behavioral and DTI approaches continue to advance, further research is warranted in this condition.

Acknowledgments

Support: This study was supported by grants P01 HD033113-12 (NICHD) and T32 MH19908

References

- Annaz D, Karmiloff-Smith A, Johnson MH, Thomas MS. A cross-syndrome study of the development of holistic face recognition in children with autism, Down syndrome, and Williams syndrome. *J Exp Child Psychol.* 2009; 102:456–486. [PubMed: 19193384]
- Barton JJ. Structure and function in acquired prosopagnosia: lessons from a series of 10 patients with brain damage. *J Neuropsychol.* 2008; 2:197–225. [PubMed: 19334311]

- Basser PJ, Mattiello J, LeBihan D. MR diffusion tensor spectroscopy and imaging. *Biophys J*. 1994; 66:259–267. [PubMed: 8130344]
- Bellugi U, Adolphs R, Cassady C, Chiles M. Towards the neural basis for hypersociability in a genetic syndrome. *Neuroreport*. 1999; 10:1653–1657. [PubMed: 10501552]
- Campbell LE, Daly E, Toal F, Stevens A, Azuma R, Karmiloff-Smith A, Murphy DG, Murphy KC. Brain structural differences associated with the behavioural phenotype in children with Williams syndrome. *Brain Res*. 2009; 1258:96–107. [PubMed: 19118537]
- Derogatis, LR. SCL-90: administration, scoring and procedures manual for the revised version and other instruments of the psychopathology rating scale series. John Hopkins University; Baltimore: 1977.
- Doyle TF, Bellugi U, Korenberg JR, Graham J. Everybody in the world is my friend” hypersociability in young children with Williams syndrome. *Am J Med Genet A*. 2004; 124:263–273.
- Duvernoy, H. *The Human Brain*. Springer Wien; New York: 1999.
- Fairhall SL, Ishai A. Effective connectivity within the distributed cortical network for face perception. *Cereb Cortex*. 2007; 17:2400–2406. [PubMed: 17190969]
- Golarai G, Hong S, Haas BW, Galaburda AM, Mills DL, Bellugi U, Grill-Spector K, Reiss AL. The fusiform face area is enlarged in Williams syndrome. *J Neurosci*. 2010; 30:6700–6712. [PubMed: 20463232]
- Grill-Spector K, Knouf N, Kanwisher N. The fusiform face area subserves face perception, not generic within-category identification. *Nat Neurosci*. 2004; 7:555–562. [PubMed: 15077112]
- Haas BW, Barnea-Goraly N, Lightbody AA, Patnaik SS, Hoefl F, Hazlett H, Piven J, Reiss AL. Early white-matter abnormalities of the ventral frontostriatal pathway in fragile X syndrome. *Dev Med Child Neurol*. 2009
- Haxby JV, Hoffman EA, Gobbini MI. The distributed human neural system for face perception. *Trends Cogn Sci*. 2000; 4:223–233. [PubMed: 10827445]
- Isaac L, Lincoln A. Featural versus configural face processing in a rare genetic disorder: Williams syndrome. *J Intellect Disabil Res*. 2011
- Jiang H, van Zijl PC, Kim J, Pearlson GD, Mori S. DtiStudio: resource program for diffusion tensor computation and fiber bundle tracking. *Comput Methods Programs Biomed*. 2006; 81:106–116. [PubMed: 16413083]
- Jones W, Bellugi U, Lai Z, Chiles M, Reilly J, Lincoln A, Adolphs R. II. Hypersociability in Williams Syndrome. *J Cogn Neurosci*. 2000; 12(Suppl 1):30–46. [PubMed: 10953232]
- Kanwisher N, McDermott J, Chun MM. The fusiform face area: a module in human extrastriate cortex specialized for face perception. *J Neurosci*. 1997; 17:4302–4311. [PubMed: 9151747]
- Karmiloff-Smith A, Thomas M, Annaz D, Humphreys K, Ewing S, Brace N, Duuren M, Pike G, Grice S, Campbell R. Exploring the Williams syndrome face-processing debate: the importance of building developmental trajectories. *J Child Psychol Psychiatry*. 2004; 45:1258–1274. [PubMed: 15335346]
- Landman BA, Farrell JA, Jones CK, Smith SA, Prince JL, Mori S. Effects of diffusion weighting schemes on the reproducibility of DTI-derived fractional anisotropy, mean diffusivity, and principal eigenvector measurements at 1.5T. *Neuroimage*. 2007; 36:1123–1138. [PubMed: 17532649]
- Lazar M. Mapping brain anatomical connectivity using white matter tractography. *NMR Biomed*. 2010; 23:821–835. [PubMed: 20886567]
- Leonard HC, Annaz D, Karmiloff-Smith A, Johnson MH. Brief report: developing spatial frequency biases for face recognition in autism and williams syndrome. *J Autism Dev Disord*. 2011; 41:968–973. [PubMed: 20945155]
- Martens MA, Wilson SJ, Reutens DC. Research Review: Williams syndrome: a critical review of the cognitive, behavioral, and neuroanatomical phenotype. *J Child Psychol Psychiatry*. 2008; 49:576–608. [PubMed: 18489677]
- Mori S, Crain BJ, Chacko VP, van Zijl PC. Three-dimensional tracking of axonal projections in the brain by magnetic resonance imaging. *Ann Neurol*. 1999; 45:265–269. [PubMed: 9989633]

- Paul LK. Developmental malformation of the corpus callosum: a review of typical callosal development and examples of developmental disorders with callosal involvement. *J Neurodev Disord.* 2011; 3:3–27. [PubMed: 21484594]
- Reiss, AL. BrainImage v5.x Software Program Center for Interdisciplinary Brain Sciences Research. Stanford University School of Medicine; 2011. <http://cibr.stanford.edu>
- Reiss AL, Hennessey JG, Rubin M, Beach L, Abrams MT, Warsofsky IS, Liu AM, Links JM. Reliability and validity of an algorithm for fuzzy tissue segmentation of MRI. *J Comput Assist Tomogr.* 1998; 22:471–479. [PubMed: 9606391]
- Riby DM, Jones N, Brown PH, Robinson LJ, Langton SR, Bruce V, Riby LM. Attention to Faces in Williams Syndrome. *J Autism Dev Disord.* 2010
- Roberts TP, Liu F, Kassner A, Mori S, Guha A. Fiber density index correlates with reduced fractional anisotropy in white matter of patients with glioblastoma. *Am J Neuroradiol.* 2005; 26:2183–2186. [PubMed: 16219820]
- Sarpal D, Buchsbaum BR, Kohn PD, Kippenhan JS, Mervis CB, Morris CA, Meyer-Lindenberg A, Berman KF. A genetic model for understanding higher order visual processing: functional interactions of the ventral visual stream in Williams syndrome. *Cereb Cortex.* 2008; 18:2402–2409. [PubMed: 18308711]
- Schaechter JD, Perdue KL, Wang R. Structural damage to the corticospinal tract correlates with bilateral sensorimotor cortex reorganization in stroke patients. *Neuroimage.* 2008; 39:1370–1382. [PubMed: 18024157]
- Sundaram SK, Kumar A, Makki MI, Behen ME, Chugani HT, Chugani DC. Diffusion tensor imaging of frontal lobe in autism spectrum disorder. *Cereb Cortex.* 2008; 18:2659–2665. [PubMed: 18359780]
- Thomas B, Eyssen M, Peeters R, Molenaers G, Van Hecke P, De Cock P, Sunaert S. Quantitative diffusion tensor imaging in cerebral palsy due to periventricular white matter injury. *Brain.* 2005; 128:2562–2577. [PubMed: 16049045]
- Thomas C, Moya L, Avidan G, Humphreys K, Jung KJ, Peterson MA, Behrmann M. Reduction in white matter connectivity, revealed by diffusion tensor imaging, may account for age-related changes in face perception. *J Cogn Neurosci.* 2008; 20:268–284. [PubMed: 18275334]
- Thompson PM, Lee AD, Dutton RA, Geaga JA, Hayashi KM, Eckert MA, Bellugi U, Galaburda AM, Korenberg JR, Mills DL, Toga AW, Reiss AL. Abnormal cortical complexity and thickness profiles mapped in Williams syndrome. *J Neurosci.* 2005; 25:4146–4158. [PubMed: 15843618]
- Tsang JM, Dougherty RF, Deutsch GK, Wandell BA, Ben-Shachar M. Frontoparietal white matter diffusion properties predict mental arithmetic skills in children. *Proc Natl Acad Sci U S A.* 2009; 106:22546–22551. [PubMed: 19948963]
- Vernooij MW, Smits M, Wielopolski PA, Houston GC, Krestin GP, van der Lugt A. Fiber density asymmetry of the arcuate fasciculus in relation to functional hemispheric language lateralization in both right- and left-handed healthy subjects: a combined fMRI and DTI study. *Neuroimage.* 2007; 35:1064–1076. [PubMed: 17320414]
- Wakana S, Jiang H, Nagae-Poetscher LM, van Zijl PC, Mori S. Fiber tract-based atlas of human white matter anatomy. *Radiology.* 2004; 230:77–87. [PubMed: 14645885]
- Woods RP, Grafton ST, Watson JDG, Sicotte NL, Mazziotta JC. Automated image registration: II. Intersubject validation of linear and nonlinear models. *J Comput Assist Tomo.* 1998; 22:153–165.
- Xia Y, Bettinger K, Shen L, Reiss AL. Automatic segmentation of the caudate nucleus from human brain MR images. *IEEE Trans Med Imaging.* 2007; 26:509–517. [PubMed: 17427738]

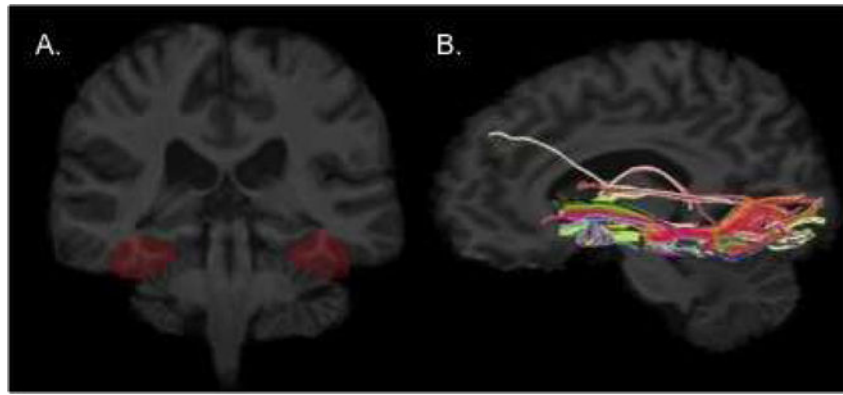


Figure 1. Regions of interest (ROIs) (A) were delineated on each participant's high-resolution spoiled gradient (SPGR) scan. The fusiform ROI included the gray and white matter between the lateral occipito-temporal sulcus, and the lateral bank of the collateral sulcus. Fibers projecting through the fusiform gyrus (B) are overlaid onto a high-resolution structural image for a TD control representative participant.

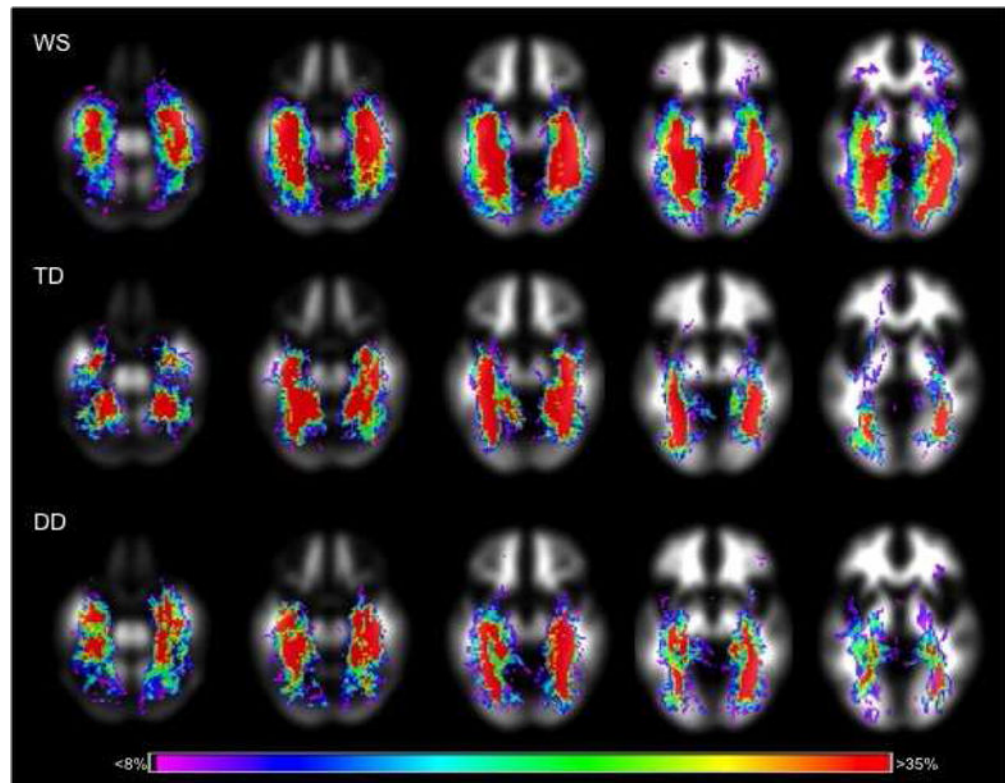


Figure 2. Probabilistic maps of reconstructed white matter fibers projecting through the fusiform gyrus in the WS (N = 20), TD (N = 10) and DD (N = 10) groups. Color scale corresponds to the relative probability of reconstructed fibers being present within each group.

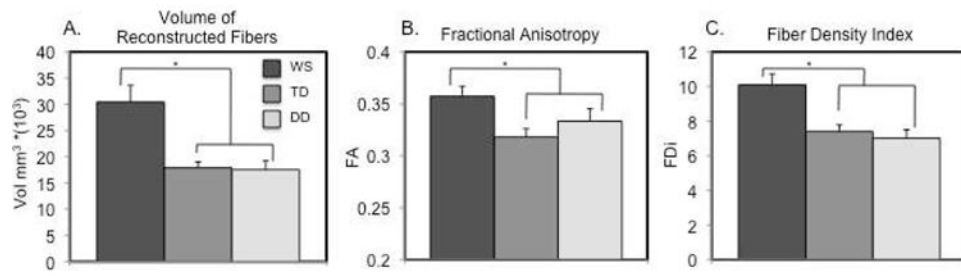


Figure 3.

Plots of macro- (A. volume of reconstructed fibers) and micro- (B. fractional anisotropy and C. fiber density index) for fibers projecting through the fusiform gyrus in WS, TD and DD participants. Vol mm = volume in millimeters, FA = fractional anisotropy, FD = fiber density, * = $p < .05$. Error bars represent standard error from the mean.